The Journal of Medicinal Plants and By-products
Original Article

Green Biosynthesis and Characterization of *Pseudomonas mendocina*-Derived Iron Nanoparticles: Antibacterial and Antibiofilm Activities Against Pathogenic Bacteria

Ismaal Jmia Abas*, Israa Najim Abdullah Al-Kaaby and Abbas Dareb Shaban

Department of Biology, College of Education-Al-Qurna, Basrah University, Basrah, Iraq

*Corresponding author: Email: ismail.abbs@uobasrah.edu.iq

Article History: Received 15 August 2026/Accepted in revised form 28 August 2026

ABSTRACT
The increasing prevalence of antimicrobial resistance and biofilm-forming bacteria has encouraged the development of alternative antimicrobial agents. This study aimed to biosynthesize iron nanoparticles (FeNPs) using the cell-free supernatant of Pseudomonas mendocina, characterize the synthesized nanoparticles, and evaluate their antibacterial and antibiofilm activities against Pseudomonas aeruginosa, Escherichia coli, Klebsiella pneumoniae, and Staphylococcus aureus. The biosynthesized FeNPs were characterized by UV–Visible spectroscopy, FT-IR, and SEM. Antibacterial activity was evaluated using the agar well diffusion method, while MIC, MBC, and antibiofilm activity were determined using standard microbiological assays. The FeNPs exhibited concentration-dependent antibacterial activity against all tested pathogens, with P. aeruginosa showing the highest susceptibility and K. pneumoniae the lowest. The MIC was 25 µg/mL for all isolates, whereas the MBC was 75 µg/mL. In addition, the nanoparticles significantly inhibited biofilm formation in all tested bacteria. These findings indicate that biosynthesized FeNPs from Pseudomonas mendocina possess promising antibacterial and antibiofilm properties and may serve as eco-friendly nanomaterials for combating biofilm-associated bacterial infections.
Keywords: Iron nanoparticles (FeNPs), *Pseudomonas mendocina,* Biosynthesis; Antibacterial activity, Antibiofilm activity, Minimum inhibitory concentration (MIC)

INTRODUCTION

It has emerged as a multidisciplinary science to provide several solutions to various problems in the fields of biomedical sciences, pharmacology, and food processing [1,2]. Nanotechnology studies fine structures ranging in size from 1 to 100 nanometers, which gives them multiple exceptional properties when compared to microscopic particles [3]. There are several ways to synthesize nanoparticles. One may be done using chemical methods, where reducing agents are used, and the second method is physical, where mineral salts are reduced by radiation, such as gamma rays or ultrasound. Most of these processes may not be environmentally friendly or may be expensive, and in most cases, it is difficult to separate the chemicals used in nanosynthesis; this is one of the disadvantages of the chemical method. Therefore, researchers resort to using biosynthesis of nanoparticles through plant extracts, bacteria, fungi, and algae. This method is effective and inexpensive [4]. Biofilms are also considered virulence factors in pathogenic bacteria against phagocytosis in the immune system. Biofilms are formed as a result of environmental changes such as lack of nutrients and accumulation of waste [5]. The formation of biofilms by bacteria will increase their resistance to antibiotics by 1000 times more than not forming them [6]. Therefore, studies have focused on eliminating bacteria that form biofilms, especially pathogenic bacteria. Therefore, one of the ways to get rid of biofilms is through the synthesis of nanoparticles by P. mendoncia bacteria. Therefore, our current study deals with the synthesis of three types of nanoparticles using iron III nitrate. Most nanosynthesis studies focus on gold and silver nanoparticles. The metallic nanoparticles of iron (III) nitrate, Fe(NO3) 3.9H2O play a great role in many applications because they show different chemical and physical properties [7], including antibacterial properties due to their very high surface area. Because of their small size, iron nanoparticles can tear the wall and pass into microorganisms [8]. Iron nanoparticles are also used in other biological fields such as pharmaceuticals and environmental purification [9]. The aim of this study is to synthesize nanoparticles from iron salts and evaluate the effectiveness of these particles in inhibiting biofilms formed by pathogenic bacteria.

MATERIALS AND METHODS

Sample Collection

55 Samples were collected from different soils (sewage, agricultural soil, and oil-polluted soil). They were collected from the north of Basra and then transferred to the laboratory. Samples were grown on culture media (nutrient agar, blood agar, and MacConky agar). On these mediums, bacteria were grown and then differentiated.

Isolation and Preliminary Identification of Bacterial Isolates

The bacteria were examined under a microscope to determine whether they were Gram-positive or Gram-negative and to determine the shapes of the bacteria. Bacterial isolates grown on different media are identified by the color of the colonies, the shape of their edges, their height, and the size of the colonies. Biochemical tests were performed to diagnose the bacteria: methyl red, catalase, oxidase, citrate, urease, and indole.

Molecular Diagnosis

DNA Extraction

Genomic DNA from Pseudomonas mendocina, used in the biosynthesis of iron nanoparticles (FeNPs), was extracted from purified bacterial isolates using the Presto™ Mini gDNA Bacteria Kit (Geneaid, Taiwan) according to the manufacturer's instructions. The quality and integrity of the extracted DNA were confirmed by agarose gel electrophoresis. Electrophoresis was performed according to the method described by Sambrook and Russell. [10] The polymerase chain reaction (PCR) products were separated on a 1.5% agarose gel prepared in Tris-acetate-EDTA (TAE) buffer, stained with ethidium bromide, and visualized under UV illumination using a gel documentation system.

Polymerase chain reaction (PCR) was performed to amplify the 16S rRNA gene of the bacterial isolate using specific primers (forward: 5′-AGAGTTTGATCMTGGCTCAG-3′ and reverse: 5′-TACGGTACCTTGTTACGACTT-3′) to achieve an amplified size of approximately 1400 base pairs, as previously described [11]. The PCR reaction was performed in a total volume of 25 µL, containing 1 µL of AccuPower PCR premix, 5 µL of template DNA, 1 µL of direct primer, 1 µL of reverse primer, and 18 µL of nuclease-free deionized water.

The amplification was carried out in the thermal cycler under the following conditions: initial denaturation at 94 °C for 5 minutes, followed by 33 cycles of denaturation at 94 °C for 40 seconds, annealing at 50 °C for 40 seconds, and extension at 72 °C for 1 minute, with a final extension step at 72 °C for 7 minutes.

Detection of Biofilm-forming Bacterial Isolates

Detection of Biofilm-Forming Bacterial Isolates Using Congo Red Agar (CRA)

The ability of the bacterial isolates to produce biofilms was initially evaluated using the Congo Red Agar (CRA) method as described by [12]. Briefly, the isolates were inoculated onto CRA plates and incubated under appropriate conditions. Biofilm production was determined based on colony morphology and color changes on the medium, where black, dry, crystalline colonies were considered indicative of biofilm-producing isolates, whereas red or pink colonies were regarded as non-biofilm producers.

Detection of Biofilm Formation by Microtiter Plate (MTP)

The biofilm-forming ability of the bacterial isolates was further quantified using the Microtiter Plate (MTP) assay according to the method described by[13]. After incubation and staining, the optical density (OD) of each well was measured at 630 nm using a Multiskan™ GO microplate reader, following the procedure described by [13]. The absorbance values were calculated as follows:

A = Absorbance of wells containing the bacterial culture.

AC = Absorbance of control wells containing culture medium only.

The biofilm-forming ability of each isolate was classified according to the following criteria:

- $A \leq AC$: Non-biofilm producer
- $AC < A \leq 2 \times AC$: Moderate biofilm producer
- $A > 2 \times AC$: Strong biofilm producer

Synthesis of Extracellular Iron Nanoparticles (FeNPs) from *Pseudomonas mendocina*

The extracellular synthesis of iron nanoparticles (FeNPs) was carried out using the cell-free supernatant of *Pseudomonas mendocina*. Briefly, the bacterial isolate was cultured in nutrient broth and incubated in a shaking incubator at 150 rpm and 37 °C for 48 h to produce sufficient biomass. The culture was then centrifuged at 6000 rpm to separate the bacterial cells, and the resulting cell-free supernatant was collected and stored at 4 °C until use. The biosynthesis of FeNPs was performed according to the method described by [14] with slight modifications. A solution of iron (III) nitrate was prepared by dissolving 0.5 g of $Fe(NO_3)_3 \cdot 9H_2O$ in 100 mL of sterile distilled water. Subsequently, 100 mL of the iron nitrate solution was mixed with 100 mL of the bacterial supernatant, resulting in an immediate colour change that indicated the formation of iron nanoparticles. The synthesized FeNPs were purified by washing three times with distilled water, followed by centrifugation at 6000 rpm for 15 min after each wash to remove unreacted materials and impurities. Finally, the purified nanoparticles were dried in a hot air oven at 100 °C for 3 h and stored for subsequent characterization and evaluation of their size, morphology, and chemical composition.

Devices and Techniques used in the Characterization of FeNPs Nanoparticles

Chromatic Change

The first indication that the biosynthesis of nanoparticles has occurred is the color change of the solution.

UV-vis Spectroscopy

1. An amount of (3) ml of the bacterial supernatant solution of *P. mendoncia* culture was taken and placed in the device, and the absorbance was determined.

2. Then, an amount of 3 mL of the solution was taken after the color change, and the device was cuvated. The absorbance was determined and compared with the absorbance of the bacterial supernatant.

FT-IR Spectrometer

An FT-IR 4600 spectrometer was used to detect the functional groups present in the bacterial supernatant solution as they were reduced by mineral salts, with accuracy and clarity (4 cm^{-1}). 0.1 mg of nanomaterials were weighed and dissolved in 10 mL of dimethyl syloxide. The nanomaterial was then placed in an ultrasonic device for 16 minutes to homogenize the material with the solvent. Then it was pipetted (5–10 lμ) and placed on the crystal lens, checked for the absence of bubbles, and pressed by the pressure arm on the sample [15].

Scanning Electron Microscope (SEM)

Another examination of nanoparticles is the use of a scanning electron microscope for surface imaging. This examination revealed the nano-shape and size distribution, and it has the ability to analyze the structure of the particles. This examination is also important in providing information about the degree of agglomeration or collection and purity of the formed particles, and modern SEM devices can determine the shape of nanoparticles under 15 nanometers. About 0.5 grams of the nanomaterial were weighed and sent to the central SEM laboratory at the University of Tehran. The nanomaterial was placed on the scanning electron microscope plate, and then the nanomaterial was covered with a layer of gold to ensure electrical conductivity [16].

Detection of Inhibitory Activity of Nanoparticles FeNPs Against Biofilm-forming Bacteria

The work was done according to method [17] (Biofilm-forming bacteria were activated on a nutrient-agar medium. Then, 5 mL of Barin Heart Infusion broth medium containing 2% glucose was prepared in test tubes. Then, the biofilm-forming bacteria were transferred to the test tubes. 100 microliters of the bacterial suspension were placed in a well of the standard plate for each bacterial isolate. Then, the first well was left without any addition of nanoparticle concentrations, so it became a control sample. Then, 100 microliters of concentrations (100 μg/mL to 50μg/mL were added to the holes in a horizontal line with three replicates for each bacterial isolate. Then the calibration plates were incubated in the incubator for 24 hours. After the incubation period was over, the contents of the holes were emptied and then washed three times with a local phosphate buffer solution to remove the bacterial cells not attached to the holes. Then crystal violet was added at a concentration of 3% to each hole of the microtiter plate and left for 15 minutes. Then 100 Mμ of 93% methanol alcohol was added, and the plate was left to dry for 10 minutes to fix the attached bacterial cells. Then, the contents of each hole were emptied and washed with distilled water to remove the non-adherent dye, and the washing was repeated three times. Then 160 Mμ of 33% glacial acetic acid was added, and the absorbance of the plate was measured at a wavelength of 630 nm using a Multiskan Go device. Then the following equation was applied to determine the amount of inhibition.

$$\text{Inhibition of biofilm formation} = \frac{\text{Wavelength of control pit} - \text{Wavelength of equation pit}}{\text{Wavelength of the control pit}} \times 100$$

Antibacterial Activity Assay

Bacterial suspensions (0.5 McFarland, approximately 1×10^8 CFU/mL) of Pseudomonas aeruginosa, Escherichia coli, Klebsiella pneumoniae, and Staphylococcus aureus were prepared from 24-h cultures grown on Nutrient Agar. The suspensions were spread onto Mueller–Hinton agar plates using sterile cotton swabs, and each isolate was tested in triplicate. Four wells (6 mm diameter) were punched into the agar. A volume of 100 μL of each FeNPs concentration was dispensed into the respective wells. Following incubation at 37 °C for 24 h, antibacterial activity was determined by measuring the diameters of the inhibition zones around each well.

Assessment of Minimum Inhibitory Concentration (MIC) and Minimum Bactericidal Concentration (MBC)

The minimum inhibitory concentration (MIC) and minimum bactericidal concentration (MBC) of the iron nanoparticles (FeNPs) were determined using the broth dilution method. Briefly, nutrient broth tube containing standardized bacterial suspensions (0.5 McFarland, approximately 1×10^8 CFU/ml) were supplemented with FeNPs at final concentrations of 25, 50, 75, and 100 μg/mL, whereas a tube without FeNPs served as the negative (growth), control After incubation at 37 °C for 24 h with shaking, the MIC was defined as the lowest concentration showing no visible bacterial growth.

To determine the MBC, aliquots (50 μL) from tubes showing no visible growth were streaked onto nutrient agar plates and incubated at 37 °C for 24 h. The MBC was recorded as the lowest FeNPs concentration that resulted in no bacterial colony growth, indicating 99.9% bacterial killing.

Statistical Analysis

All experiments were performed in triplicate (n = 3). Data were expressed as mean ± standard deviation (SD). Statistical differences between concentrations were evaluated using one-way and two-way analysis of variance (ANOVA) in IBM SPSS Statistics version 27. Differences were considered statistically significant at $p < 0.05$.

RESULTS and DISCUSSION

Sample Collection

Samples were collected from 9/1/2025 to 11/1/2025 from various areas of northern Basra, totaling 55 samples. The laboratory culture results showed that the number of samples in which growth occurred was 28 positive culture samples, and the number of samples in which no growth occurred was 27 negative culture samples**.**

Diagnosis

Microscopic Diagnosis

All bacterial isolates were purified, and staining of the bacteria showed that most of the bacteria were Gram-negative, i.e., 10 positive isolates (35.7%) and 18 negative isolates (64.3%).

Phenotypic Diagnosis

I relied on the phenotypic characteristics for the initial diagnosis, as the shape, color, smell, texture, and size of the growing colonies were observed on the culture media of nutrient agar, blood agar, and MacConkey agar.

Biochemical Tests

Biochemical tests were performed, and the test results were as shown in the table 1.

Table 1 shows the biochemical tests.

Bacteria	Oxidase	MR	VP	Urease	H_2S production	citrate	Gas production	Indole	Coagulase
P. mendoncia	+	+	-	-	-	+	-	-	-

Molecular Diagnosis

Molecular identification of the bacterial isolates under study was carried out, and the PCR technique for the 16S rRNA gene was used to identify the bacteria. The results of the DNA extraction of the bacteria showed the appearance of DNA bands that were extracted from the bacteria.

Polymerase Chain Reaction (PCR)

After extracting the DNA from the bacterial isolates, the DNA was amplified using polymerase chain reaction (PCR). The amplification results showed that the DNA was 1400 bp in size when compared with the DNA ladder, as shown in figure 1.

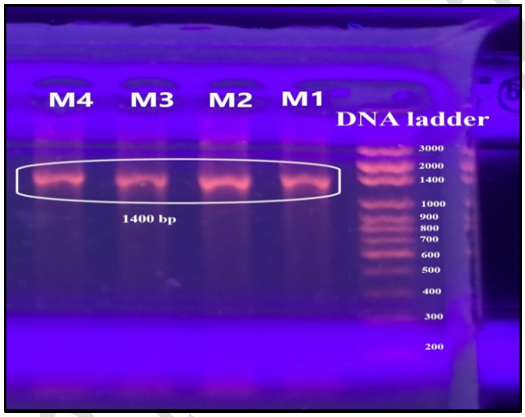

Fig. 1 shows the DNA size of bacterial isolates and its comparison with the DNA ladder size index.

Genetic Sequencing Analysis

The purified PCR product was subjected to Sanger sequencing, and the resulting 16S rRNA gene sequence was compared with sequences deposited in the NCBI database using BLAST.

Biosynthesis of Nanoparticles

The present study showed that *P. mendoncia* bacteria have the ability to biosynthesize nanoparticles of FeNPs. The properties of the synthesized nanoparticles were confirmed using the following techniques:

Color Change

The first observation of nanobiosynthesis is the color change. The color change of Iron nanoparticles was observed from yellow to brown, and this study was consistent with what was reported by [18].

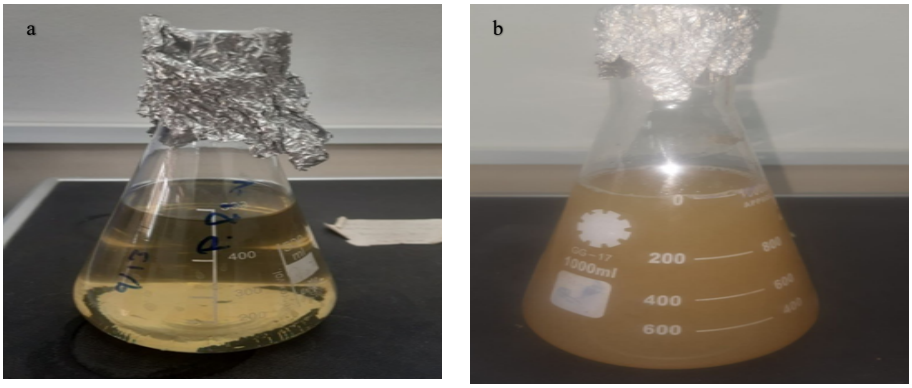

Fig. 2 shows the color variation in solutions for each of the following:

A. a-Bacterial suspension

B. b- Color change in iron (III) nitrate solution

UV-visible Spectrometer

The next step to verify the synthesis of nanoparticles is to measure the wavelength, as each nanomaterial has a specific wavelength. The absorption peak of iron nanoparticles was at a wavelength of 304 nanometers, as shown in figure 3. The results of this study were identical to those of study [19]. It was shown that proteins and enzymes, especially the reduction enzyme found in the supernatant solution of bacterial cultures, play a major role in the biosynthesis of nanoparticles [20]. The formation of nanoparticles in a biological way, whether outside or inside the cells, depends on the location of the formation of these particles. Bacteria work to attract metal ions present in the environment and also convert metal ions into elements through their enzymes, which are formed as a result of biological activities [21].

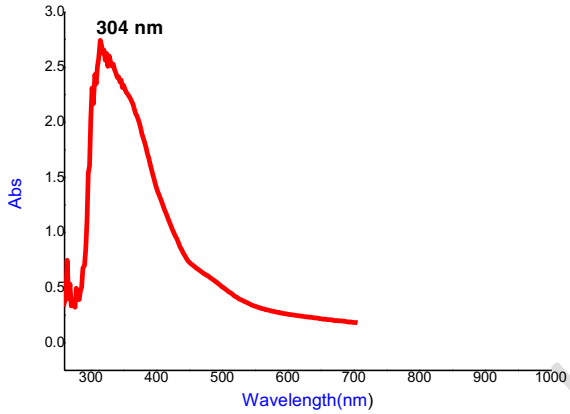

Fig. 3 UV-visible spectra of FeNPs nanoparticles produced by *P. mendoncia*

Fourier Transform Infrared (FTIR) Analysis of Biosynthesized FeNPs

The FTIR spectrum of the biosynthesized iron nanoparticles (FeNPs) revealed several characteristic absorption bands, indicating the presence of different biomolecules involved in the reduction and stabilization of the nanoparticles (Fig. 4). Broad absorption bands observed at 3833.79, 3741.23, 3617.80, and 3274.54 cm^{-1} were attributed to O–H and N–H stretching vibrations, suggesting the presence of hydroxyl and amine groups derived from proteins, amino acids, polysaccharides, and other extracellular metabolites produced by Pseudomonas mendocina [22].

The absorption band at 2919.70 cm^{-1} corresponds to C–H stretching vibrations of aliphatic hydrocarbons, indicating the presence of lipid or protein components associated with the nanoparticle surface. A distinct peak at 2360.44 cm^{-1} was assigned to carbonyl-related stretching vibrations, which may originate from carboxyl-containing biomolecules participating in metal ion chelation. The strong band at 1643.05 cm^{-1} was attributed to C=O stretching (amide I) or C=C stretching vibrations, reflecting the involvement of proteins and other organic compounds in nanoparticle formation. In addition, the absorption peak at 1538.92 cm^{-1} corresponds to N–O stretching vibrations, while the band at 1461.78 cm^{-1} is associated with C–H bending vibrations, confirming the presence of proteinaceous compounds surrounding the nanoparticles.

The absorption peak observed at 960.38 cm^{-1} is assigned to O–H bending or C–O stretching vibrations, indicating alcohols or polysaccharides that may contribute to nanoparticle stabilization. Furthermore, the low-frequency bands around 540 and 440 cm^{-1} may be associated with Fe–O vibrations, supporting the presence of iron-containing oxide phases.

The FTIR analysis demonstrates that extracellular biomolecules secreted by *Pseudomonas mendocina* served a dual role as reducing and capping agents during nanoparticle biosynthesis. Hydroxyl, amine, carbonyl, and carboxyl functional groups facilitated the reduction of ferric ions and prevented nanoparticle aggregation by forming a protective organic layer around the particle surface. Similar FTIR profiles have been reported for biologically synthesized iron nanoparticles using bacterial and fungal extracts, where proteins, enzymes, and extracellular polysaccharides were identified as the principal biomolecules responsible for nanoparticle formation and stability [23,24].

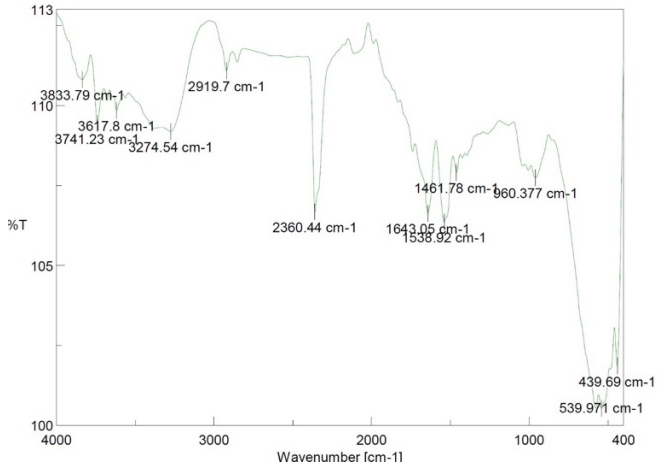

Fig. 4 FTIR spectrum showing the functional groups associated with biosynthesized iron nanoparticles (FeNPs).

SEM Examination

The shape, size, and surface morphology of the particles were determined by scanning electron microscopy. The electron microscope images of iron nanoparticles showed that they have multiple shapes, but the spherical shape predominated and the size ranged from (D1 = 29.82) as in figures 5. The electron microscope image showed that they have smooth levels with a uniform shape in the form of secondary iron centers, and the reason for the increase in the size of the smaller particles may be at high temperatures. At low temperatures, they lead to better connections between the secondary particles, and as a result, the shape of the secondary particles may change to a spherical shell. The results of the current study were consistent with Study [23].

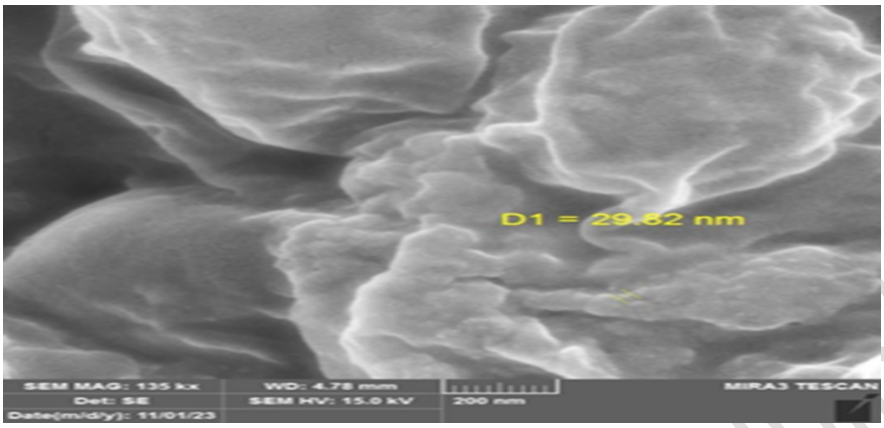

Fig. 5 Electron Microscope of Iron Nanoparticles

Detection of Biofilm Formation in Pathological Bacteria

The detection of biofilm-forming bacteria, which is considered a virulence factor, was carried out for four types of bacteria, namely *E. coli, K. penumonae, P. aeruginosa,* and *S. aureus*, using two methods:

Congo Red Method

The bacteria were cultured on Congo red medium, the aim of which was to detect whether the bacteria formed biofilms or not. The results showed that this method formed black colonies, indicating that the bacteria formed biofilms with high intensity, as shown in figures 6. The results of this study agreed with [16].

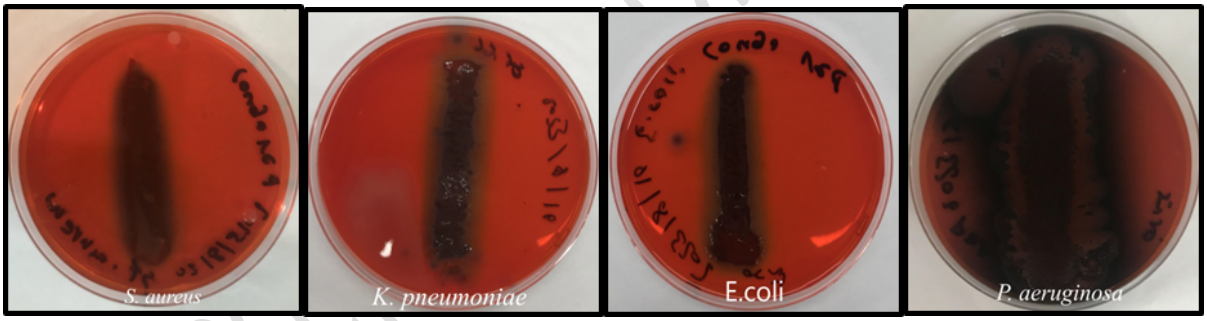

Fig. 6 Detection of biofilms in pathogenic bacteria using Congo red agar.

Detection of biofilms by a standard plate (Microtiter plate)

Biofilm-forming bacteria were detected using a microtiter plate. The ELISA results showed that, by comparing the reading of the negative control well (i.e., the well containing only culture medium) with the reading of the positive control well (i.e., the well containing culture medium and bacterial colonies), as shown in figures 7. The calculation of the intensity of biofilm formation showed that all four isolates formed biofilms with high intensity, as shown in Table 8. This study was consistent with what was reported by [15].

Table 3 Intensity of biofilm formation in pathogenic bacterial isolates by microtiter plate

Bacteria	Biofilm intensity calculation equation		Biofilm intensity
P. aeruginosa	2 * AC ≤ A	2 * 0.097 ≤ 1.135	Strong biofilm
E.coli	2 * AC ≤ A	2 * 0.073 ≤ 1.511	Strong biofilm
K. pneumoniae	2 * AC ≤ A	2 * 0.096 ≤ 1.164	Strong biofilm
S. aureus	2 * AC ≤ A	2 * 0.106 ≤ 1.327	Strong biofilm

Measurement of the Inhibitory Activity of Nanoparticles Against Biofilm-forming Bacteria Using a Titration Plate

The antibiofilm activity of FeNPs was evaluated against four pathogenic bacteria at two concentrations (50 and 100 µg/mL). Data were expressed as mean ± standard deviation (SD) from three independent replicates. A two-way analysis of variance (ANOVA) was performed to determine the effects of bacterial species and nanoparticle concentration.

The inhibition percentages ranged from 89.73 ± 0.19% to 91.81 ± 0.61%. The highest inhibition was observed at 100 µg/mL for *P. aeruginosa* and *S. aureus* (91.81%), whereas the lowest value was recorded for *S. aureus* at 50 µg/mL (89.73%). Two-way ANOVA

revealed that nanoparticle concentration had a highly significant effect on antibiofilm activity ($F = 186.4$, $df = 1$, $p < 0.0001$). In contrast, the effect of bacterial species was not statistically significant ($F = 2.31$, $df = 3$, $p = 0.11$), and the interaction between bacterial species and concentration was also non-significant ($F = 1.42$, $df = 3$, $p = 0.27$). These results indicate that increasing the FeNP concentration from 50 to 100 µg/mL significantly enhanced biofilm inhibition regardless of the bacterial species tested. The difference in inhibition of biofilms may be due to the different interactions between iron nanoparticles and bacteria, and the susceptibility of bacteria used in this study to the effect may differ [25]. The main mechanism of toxicity of iron nanoparticles is related to metal oxides, as they carry a positive charge, although bacteria carry a negative charge. This may lead to an electromagnetic interaction between iron oxides and bacteria, which results in oxidation and thus the death of bacteria. Iron particles have a bactericidal effect, which is of great importance as it acts as an antibacterial against disease-causing bacteria [26,27].

Table 4 Antibiofilm activity (%) of FeNPs against pathogenic bacteria

Bacteria	50 µg/mL (Mean ± SD)	100 µg/mL (Mean ± SD)
P. aeruginosa	90.19 ± 0.20	91.81 ± 0.61
E. coli	90.21 ± 0.17	91.66 ± 0.20
K. pneumoniae	90.01 ± 0.24	91.72 ± 0.15
S. aureus	89.73 ± 0.19	91.81 ± 0.15

Values represent mean ± standard deviation (n = 3)

Antibacterial Activity of Iron Nanoparticles (FeNPs)

The antibacterial activity of biosynthesized Iron nanoparticles (FeNPs) was determined against four clinically important pathogenic bacteria, *Pseudomonas aeruginosa*, *Escherichia coli*, *Klebsiella pneumoniae*, and *Staphylococcus aureus*, using the agar well diffusion method. All FeNPs exhibited inhibitory activity against the tested bacteria, with inhibition zones increasing in a concentration-dependent manner. The inhibition zone data were expressed as mean ± standard deviation (SD) based on three independent replicates (n = 3). A two-way analysis of variance (ANOVA) was performed to evaluate the effects of FeNP concentration and bacterial species, as well as their interaction, on the inhibition zone diameter (able 5 and Fig. 7). The greatest antibacterial activity was generally observed at 100 µg/mL, whereas the lowest inhibition was recorded at 25 µg/mL. Among the tested isolates, *P. aeruginosa* was the most susceptible, whereas *K. pneumoniae* exhibited the lowest susceptibility to FeNPs show in figure 7 Two-way ANOVA revealed significant effects of bacterial species ($F_{3,32} = 15.504$, $p < 0.001$) and FeNP concentration ($F_{3,32} = 245.917$, $p < 0.001$), as well as a significant bacterial species × concentration interaction ($F_{9,32} = 5.529$, $p < 0.001$). The antibacterial activities obtained in the present study were consistent with previous reports describing the efficacy of biologically synthesized FeNPs against both Gram-positive and Gram-negative bacteria [28, 29]. Minor differences in inhibition zone diameters among studies may be attributed to variations in nanoparticle size, morphology, concentration, synthesis method, and bacterial strain.

Table 5 Antibacterial Activity of Iron Nanoparticles (FeNPs)

Bacterium	25 µg/mL	50 µg/mL	75 µg/mL	100 µg/mL
P. aeruginosa	10.2 ± 0.6	13.8 ± 0.6	16.4± 0.6	20.0 ± 1.0
E. coli	9.8 ± 0.6	12.2 ± 0.6	15.1 ± 1.0	18.4 ± 0.6
K. pneumoniae	12.1 ± 1.0	13.4 ± 0.6	14.8 ± 0.6	16.6 ± 0.6
S. aureus	11.8 ± 0.6	14.4 ± 0.6	17.1 ± 1.0	19.4 ± 0.6

Values represent mean ± standard deviation (n = 3)

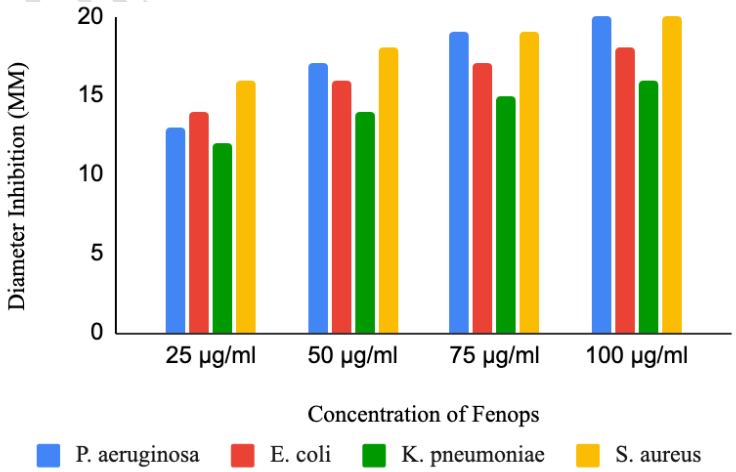

Fig. 7 show Antibacterial Activity of Iron Nanoparticles (FeNPs)

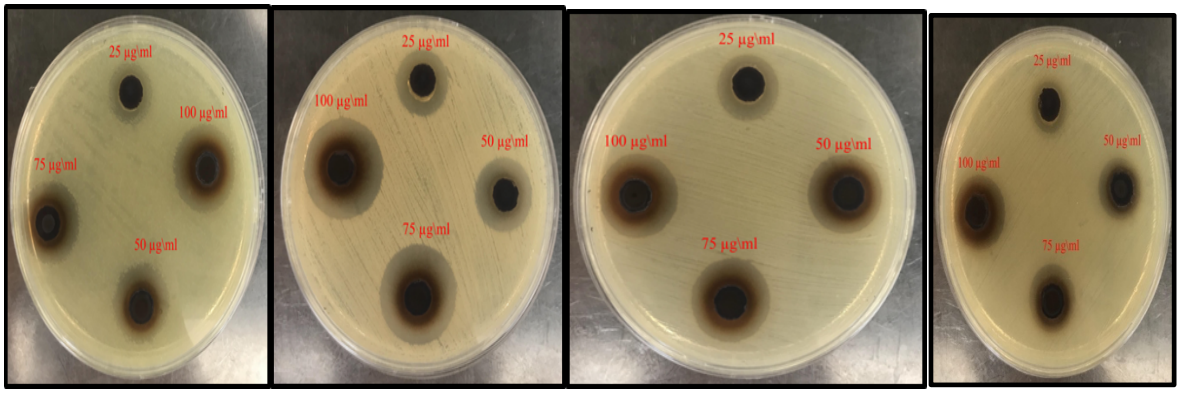

Fig. 8 show inhibition zone of FeNps on bacteria

Minimum Inhibitory Concentration (MIC) and Minimum Bactericidal Concentration (MBC)

The MIC and MBC of biosynthesized Iron nanoparticles (FeNPs) produced by *Pseudomonas* modecina were evaluated against *P. aeruginosa*, *E. coli*, *Klebsiella pneumoniae*, and *Staphylococcus aureus*. The MIC was consistently 25 µg/mL for all tested bacterial isolates, regardless of the bacterial source used for FeNP synthesis. The MBC values were 75 µg/mLfor all isolates. These findings agree with previous reports demonstrating MIC values of 16–35 µg/mL and MBC values of 55–100 µg/mL for biosynthesized FeNPs against similar pathogenic bacteria [30]. The detailed MIC and MBC values are presented in table 5.

Table 6 Minimum Inhibitory Concentration (MIC) and Minimum Bactericidal Concentration (MBC) of Biosynthesized Iron Nanoparticles (FeNPs)

Type of bacteria	Minimum Inhibitory Concentration (MIC) and Minimum Bactericidal Concentration (MBC) of Biosynthesized Iron Nanoparticles (FeNPs)	
	MIC	MBC
P. aeruginosa	25µg\ml	75 µg\ml
E.coli	25 µg\ml	75 µg\ml
K. pneumoniae	25 µg\ml	75 µg\ml
S. aureus	25 µg\ml	75 µg\ml

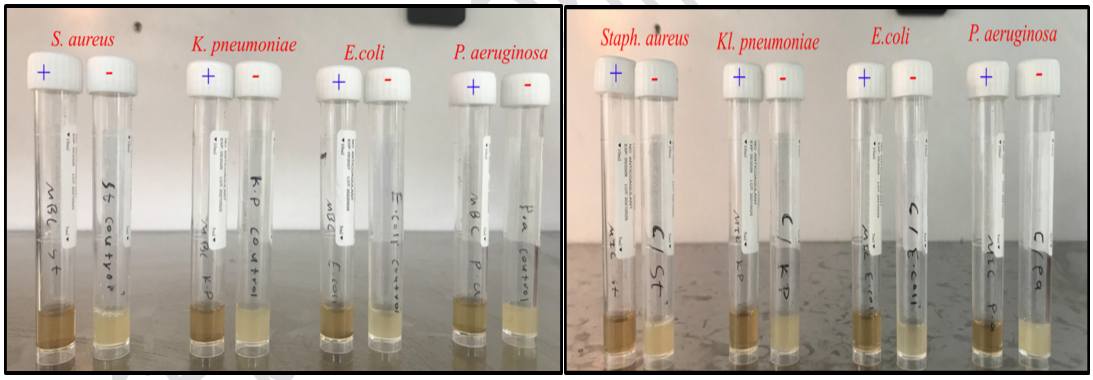

Fig. 9 Minimum Inhibitory Concentration (MIC) and Minimum Bactericidal Concentration (MBC)

CONCLUSION

Iron nanoparticles (FeNPs) were successfully biosynthesized using the cell-free supernatant of Pseudomonas mendocina and confirmed by physicochemical characterization. The biosynthesized FeNPs exhibited significant concentration-dependent antibacterial and antibiofilm activities against *Pseudomonas aeruginosa, Escherichia coli, Klebsiella pneumoniae,* and *Staphylococcus aureus*, with a MIC of 25 µg/mL and an MBC of 75 µg/mL. These findings suggest that biosynthesized FeNPs are promising eco-friendly antimicrobial nanomaterials for controlling biofilm-associated bacterial infections.

Consent for Publication

Not Applicable.

Data Availability

The data generated and/or analyzed during the current study are available from the corresponding author upon reasonable request.

Conflict of Interest

The author declare that they have no known financial or personal conflicts of interest that could have appeared to influence the work reported in this paper**.**

Funding

The authors received no financial support for this research, authorship, or publication.

Authors' Contributions

I contributed to the conception and design of the study, data collection and analysis, interpretation of the results, and preparation and revision of the manuscript. I read and approved the final version of the manuscript.

Acknowledgement

The author would like to express their sincere appreciation to the Department of Biology, College of Education Al-Qurna, University of Basrah, Basrah, Iraq, for providing the laboratory facilities and technical support necessary to conduct this research. The author also acknowledges the assistance of all laboratory staff who contributed to the successful completion of this study**.**

REFERENCES

1. Malik S., Muhammad K., Waheed Y. Emerging applications of nanotechnology in healthcare and medicine. Molecules. 2023;28(18):6624.
2. Modi S., Prajapati R., Inwati G.K., Deepa N., Tirth V., Yadav V.K., et al. Recent trends in fascinating applications of nanotechnology in allied health sciences. Crystals. 2021;12(1):39.
3. Binns C. Introduction to nanoscience and nanotechnology. John Wiley & Sons. 2021.
4. Salem S.S., Fouda A. Green synthesis of metallic nanoparticles and their prospective biotechnological applications: an overview. Biological Trace Element Research. 2021;199(1):344-370.
5. Ramírez-Larrota J.S., Eckhard U. An introduction to bacterial biofilms and their proteases, and their roles in host infection and immune evasion. Biomolecules. 2022;12(2):306.
6. Abebe G.M. The role of bacterial biofilm in antibiotic resistance and food contamination. International Journal of Microbiology. 2020;2020(1):1705814.
7. Alghamdi H.M., Abutalib M., Rajeh A., Mannaa M.A., Nur O., Abdelrazek E. Effect of the Fe2O3/TiO2 nanoparticles on the structural, mechanical, electrical properties and antibacterial activity of the biodegradable chitosan/polyvinyl alcohol blend for food packaging. Journal of Polymers and the Environment. 2022;30(9):3865-3874.
8. Zúñiga-Miranda J., Guerra J., Mueller A., Mayorga-Ramos A., Carrera-Pacheco S.E., Barba-Ostria C., et al. Iron oxide nanoparticles: green synthesis and their antimicrobial activity. Nanomaterials. 2023;13(22):2919.
9. Verma C., Verma D.K., Berdimurodov E., Barsoum I., Alfantazi A., Hussain C.M. Green magnetic nanoparticles: a comprehensive review of recent progress in biomedical and environmental applications. Journal of Materials Science. 2024;59(2):325-358.
10. Green M.R., Sambrook J. Analysis of DNA by agarose gel electrophoresis. Cold Spring Harbor Protocols. 2019;2019(1):pdb.top100388.
11. Barghouthi S.A. A universal method for the identification of bacteria based on general PCR primers. Indian Journal of Microbiology. 2011;51(4):430-444.
12. Mori S., Yamada A., Kawai K. Evaluation of the biofilm detection capacity of the Congo Red Agar method for bovine mastitis-causing bacteria. Japanese Journal of Veterinary Research. 2024;71(3):109-116.
13. Abdelraheem W., Abdelraheem S., Zaki S. Phenotypic and genotypic detection of biofilm formation and methicillin resistance among Staphylococcus aureus isolates. Microbes and Infectious Diseases. 2021;2(3):485-496.
14. Ashrafi-Saiedlou S., Rasouli-Sadaghiani M., Fattahi M., Ghosta Y. Biosynthesis and characterization of iron oxide nanoparticles fabricated using cell-free supernatant of Pseudomonas fluorescens for antibacterial, antifungal, antioxidant, and photocatalytic applications. Scientific Reports. 2025;15(1):1018.
15. Kamnev A.A., Dyatlova Y.A., Kenzhegulov O.A., Vladimirova A.A., Mamchenkova P.V., Tugarova A.V. Fourier transform infrared (FTIR) spectroscopic analyses of microbiological samples and biogenic selenium nanoparticles of microbial origin: sample preparation effects. Molecules. 2021;26(4):1146.
16. Tommalieh M., Ibrahium H.A., Awwad N.S., Menazea A. Gold nanoparticles doped polyvinyl alcohol/chitosan blend via laser ablation for electrical conductivity enhancement. Journal of Molecular Structure. 2020;1221:128814.
17. Majumdar M., Khan S.A., Nandi N.B., Roy S., Panja A.S., Roy D.N., et al. Green synthesis of iron nanoparticles for investigation of biofilm inhibition property. ChemistrySelect. 2020;5(43):13575-13583.
18. Fahmy H.M., Mohamed F.M., Marzouq M.H., Mustafa A.B.E-D., Alsoudi A.M., Ali O.A., et al. Review of green methods of iron nanoparticles synthesis and applications. BioNanoScience. 2018;8(2):491-503.
19. Taha A.B., Essa M.S., Chiad B.T. Spectroscopic study of iron oxide nanoparticles synthesized via hydrothermal method. Chemical Methodologies. 2022;6(12):977-984.
20. Iravani S. Bacteria in nanoparticle synthesis: current status and future prospects. International Scholarly Research Notices. 2014;2014(1):359316.
21. Qin W., Wang C.Y., Ma Y.X., Shen M.J., Li J., Jiao K., et al. Microbe-mediated extracellular and intracellular mineralization: environmental, industrial, and biotechnological applications. Advanced Materials. 2020;32(22):1907833.
22. Hafiz N.A., Zainurin A.S.A., Hashib S.A., Osman M.S., So'aib M.S., Lenggoro I.W., *et al*. Green synthesis of chitosan-coated iron oxide nanoparticles using pineapple peel extract: a sustainable approach. AIP Conference Proceedings. 2026.
23. Yadav A., Theivasanthi T., Paul P., Upadhyay K. Extracellular biosynthesis of silver nanoparticles from plant growth promoting rhizobacteria Pseudomonas sp. arXiv preprint arXiv:1511.03130. 2015.
24. Ovais M., Khalil A.T., Islam N.U., Ahmad I., Ayaz M., Saravanan M., et al. Role of plant phytochemicals and microbial enzymes in biosynthesis of metallic nanoparticles. Applied Microbiology and Biotechnology. 2018;102(16):6799-6814.
25. Shkodenko L., Kassirov I., Koshel E. Metal oxide nanoparticles against bacterial biofilms: perspectives and limitations. Microorganisms. 2020;8(10):1545.
26. Sadek A.H., Asker M.S., Abdelhamid S.A. Bacteriostatic impact of nanoscale zero-valent iron against pathogenic bacteria in the municipal wastewater. Biologia. 2021;76(9):2785-2809.
27. Wahab S., Salman A., Khan Z., Khan S., Krishnaraj C., Yun S.I. Metallic nanoparticles: a promising arsenal against antimicrobial resistance—unraveling mechanisms and enhancing medication efficacy. International Journal of Molecular Sciences. 2023;24(19):14897.
28. Kayani R., Rustam A., Saleem U., Bilal M., Bakhtiyar M., Jamshaid S., et al. Chlorophytum comosum-mediated iron nanoparticles: an eco-friendly approach for antimicrobial and dye degradation applications. Bulletin of Biological and Allied Sciences Research. 2025;2025(1):94.
29. Padilla-Cruz A.L., Garza-Cervantes J.A., Vasto-Anzaldo X.G., García-Rivas G., León-Buitimea A., Morones-Ramírez J.R. Synthesis and design of Ag-Fe bimetallic nanoparticles as antimicrobial synergistic combination therapies against clinically relevant pathogens. Scientific Reports. 2021;11(1):5351.

30. Ahmadi S., Fazilati M., Nazem H., Mousavi S.M. Green synthesis of magnetic nanoparticles using Satureja hortensis essential oil toward superior antibacterial/fungal and anticancer performance. BioMed Research International. 2021;2021(1):8822645.